Using deep learning and radar backscatter for mapping river water surface

Diana Orlandi[1], Federico A. Galatolo[1], Mario C. G. A. Cimino[1],
Carolina Pagli[2], Nicola Perilli[3], Joao A. Pompeu[4], Itxaso Ruiz[4]
[1]*Dept. of Information Engineering, University of Pisa, Italy*
[2]*Dept. of Earth Science, University of Pisa, Italy*
[3]*Dept. of Civil and Industrial Engineering, University of Pisa, Italy*
[4]*BC3, Basque Centre for Climate Change, Leioa, Spain*
diana.orlandi@phd.unipi.it, federico.galatolo@ing.unipi.it, {mario.cimino, carolina.pagli, nicola.perilli}@unipi.it, {itxaso.ruiz, joao.pompeu}@bc3research.org

Keywords: Hydrological Remote Sensing, River Water Surface Mapping, Radar Backscatter, Convolutional Neural Network, Attention.

Abstract: In the last decades, the effects of global warming combined with growing anthropogenic activities have caused a mismatch in the water supply-demand, resulting in a negative impact on numerous Mediterranean rivers regime and on the functionality of related ecosystem services. Thus, for water management and mitigation of the potential hazards, it is fundamental to efficiently map areal extents of river water surface. Synthetic Aperture Radar (SAR) is one of the satellite technologies applied for hydrological studies, but it has a spatial resolution which is limited for the study of rivers. On the other side, deep learning technology exhibits a high modelling potential with low spatial resolution data. In this paper, a method based on convolutional neural networks is applied to the SAR backscatter coefficient for detecting river water surface. Our experimental study focuses on the lower reach of Mijares river (Eastern Spain), covering a period from Apr 2019 to Sept 2022. Results suggest that radar backscattering has high potential in modelling water river trends, contributing to the monitoring of the effects of climate change and impacts on related ecosystem services. To assess the effectiveness of the method, the output has been validated with the Normalized Difference Water Index (NDWI).

1 INTRODUCTION

In hydrology, the ability to regularly assess the river water surface is of utmost importance for several purposes: water accountability, water allocation, flooding mitigation, and the reinforcement of the ecosystem services. In the literature, satellite based remote sensing has been used to monitor the areal extent of surface water bodies (Frappart *et al.*, 2021; Botha *et al.*, 2020). Most of the research focuses on studying flooding events (Carreño-Conde *et al.*, 2019; Quiròs and Gagnon, 2022; Tran *et al.*, 2022), while the monitoring of the areal extent of river water surface is a more complex task, with fewer studies (Filippucci *et al.*, 2022). Specifically, remote sensing data include different technologies, ranging from radar to multispectral. Radar data is not affected by weather conditions (e.g. clouds) while it is by vegetation. In particular, this is relevant for the monitoring of the extents of water in narrow river, given the limited number of water pixels. In contrast, the spatial resolution provided by multispectral satellites, especially for optical bands (such as Sentinel-2 used in this study), is higher than resolution of Sentinel-1 SAR data. For this reason, the Synthetic Aperture Radar (SAR) is less used to map the extent of river water surface respect to the optical data.

On the other hand, there is a high potential in deep learning technology for its capabilities of mapping and image features identification (Ronneberger *et al.*, 2015), also applied to SAR data under low resolution conditions (Jiang *et al.*, 2022; Orlandi *et al.*, 2022). Specifically, the U-Net convolutional neural network has been recently experimented for the mapping of the extent of lake water surface. U-Net carries out the semantic segmentation task, partitioning the image into different regions, for corresponding classes (e.g.

surface water, *vegetation*, and so on) (Ronneberger *et al.*, 2015). In the context of image segmentation, U-Net is equipped with a spatial attention mechanism, to highlight only the relevant parts of the image during training. As a result, the computational resources on the irrelevant part of the image are low, with better generalisation capability.

In this paper, a U-Net architecture is used on the radar backscatter coefficient with the purpose of efficiently identifying and mapping areal extents of river water surface. Satellite multispectral data are used for validating the method. The paper is structured as follows. Section 2 discusses the case study, i.e., the area and the data sets achieved. Section 3 covers the overall methods in terms of Multispectral data pre-processing, SAR data pre-processing, and U-Net segmentation. Experimental results are discussed in Section 4. Finally, Section 4 draws also the conclusions.

2 CASE STUDY

2.1 Study area

The study area (Figure 1) focuses on the last 20 km of the Mijares river in Eastern Spain (Pompeu *et al.*, 2021). Along the river path there are the Arenoso (93 Mm^3), Sichar (49 Mm^3) and Maria Cristina (18.4 hm^3) reservoirs, which support the agricultural needs and guarantee the water supply to the Sichar dam (0.2 Mm^3) downstream (Macian-Sorribes *et al.*, 2015). In the lower reach of the Mijares river (Figure 1), the alluvial plain is characterized by meandering sequence of fine to coarse sediments, which grade to deltaic successions in the Almazora and Buriana plains. In the last decades, the region has experienced hotter seasons, a concentration of the total annual rainfall (MedECC, 2020), and an overall decrease of precipitation in the period 1980-2012 with respect to the period 1940-2012 in 3-7%. Overall, the area has available water resources of 335.7 hm^3/year and a water demands of 268.23 hm^3/year (Confederación Hidrográfica del Júcar, 2019). There are records historically significant torrential floods that could not be correctly gauged, which are only expected to rise given the increasingly unstable weather patterns forecasted for the watershed (Masson-Delmotte *et al.*, 2021).

2.2 Datasets

Our data sets consist of images acquired by Sentinel-2 and Sentinel-1A satellites, provided by the European Space Agency (ESA). Sentinel-2 is a Multispectral satellite, acquiring images in 13 bands. For this work, we used 36 Level-1C images (Table 1) covering a period from October 2019 to August 2022, considering all the 13 bands but also selecting particular bands, such as B3 and B8 (visible and near-infrared, respectively) to build a river mask. Sentinel-1A is a SAR satellite operating in the C-band. We used 104 Single Look Complex (SLC) images, acquired in Descending orbit and in Interferometric Wide swath beam mode (Table 1), covering the time period from April 2019 to September 2022.

Table 1: SAR and Multispectral datasets.

Satellite	Sentinel-1A	Sentinel-2
Product Level	Single Look Complex (SLC)	Multispectral Instrument (MSI) - Level-1C
Tiles	-	T31TBE, T30TYK
Spatial Resolution (m)	20 × 20	10 × 10
Orbit	Descending (path 8, frame 458)	-
Acquisition mode	Interferometric Wide swath (IW)	-
Revisit time	12 days	-
Polarization	VV	-

3 METHODS

3.1 Multispectral images pre-processing

To identify the areal extent of the river water surface the NDWI is computed, i.e., a satellite-derived index utilizing visible and near-infrared wavelengths not affected by meteorological conditions (e.g. Tran *et al.*, 2022). Specifically, NDWI has been computed on 36 Sentinel-2 images, using band 3 (visible) and 8 (near-infrared) through the following formula:

$$NDWI = \frac{B3 - B8}{B3 + B8} \quad (1)$$

Then, based on the NDWI, a polygon of the areal extent of the water has been created for each image. This process has been also validated by comparing each polygon to all the 13 bands in the image. Thus, the final Water Surface Mask (WSM) has been created by comparing the 36 different water polygons generated. As a final step, in order to give to the U-Net architecture some validation multispectral maps to train the network, the 36 different NDWI maps have been translated into binary images. Each pixel

of a binary image is set to 0 outside the WSM, and 1 to mark the presence of water within the final WSM, where the selection of the threshold water/non-water set to -0.1 (Figure 2) has been validated comparing with all the bands of the Multispectral images. The column on the right in Figure 2 shows the flow chart.

3.2 SAR images pre-processing

A series of 104 SAR images have been processed to obtain the backscatter coefficient from the raw radar images. Figure 2 left shows the workflow. First, the thermal noise removal has been applied, choosing the VV (Vertical-Vertical) polarization. This option was preferred, instead of VH polarization. Indeed, differently from other works focused on floodings events (Carreño-Conde *et al.*, 2019; Tran *et al.*, 2022), in this research the general scarce presence of water requires a stronger backscatter value provided by VV polarization. The following step was the radiometric calibration. To achieve a radiometrically calibrated backscatter, σ is set to 0, from the amplitudes stored in the SLC image. Subsequently, the azimuth debursting is carried out to merge all bursts using the TOPSAR-Deburst method, followed by the Multilook step with a window size of 1×1 in Range and Azimuth, respectively. Figure 3 shows three different filters that have been tested to remove the remaining speckle: Lee, IDAN and Lee Sigma. Differently from other works (e.g. Carreño-Conde *et al.*, 2019), in this study, in terms of accuracy and better visual estimation of the presence of water, the Lee Sigma filter gives the best results, compared to both Lee which appears noisier and to IDAN that provides less details. Then, the image is projected from Slant Range onto Ground Range (SRGR). Finally, the Terrain-Correction geocoding has been applied using the Digital Elevation Model of the NASA Shuttle Radar Topography Mission 1 arcsec of 30 m spatial resolution.

3.3 SAR image semantic segmentation

Overall, the task of detecting the river water surface is tackled as a SAR image segmentation task. Specifically, a 128×128-pixel SAR image is considered as an input. A particular Convolutional Neural Network, known as U-Net (Ronneberger *et al.*, 2015) is used for the SAR image segmentation task. A U-Net consists of a contracting and an expanding path, to capture context and precise localization, respectively. A U-Net can be trained from very few images, outperforming the other approaches (Qin *et al.*, 2020).

Figure 4 shows two examples of image segmentation, after 100 training iterations (images a-e), and after 30,000 training iterations (f-j) of the U-Net. Specifically, image (a) and (f) are two examples of raw input. Second, the known WSM has been used to filter the initial raw input (b and g). Third, the reference truth data (c) and (h) are derived from the Multispectral images. Fourth, images (d) and (i) show the output provided by the U-Net. Finally, images (e) and (j) represent the binarized water/non-water outputs: pixel values larger or equal than 0.5 are set to 1, otherwise they are set to 0.

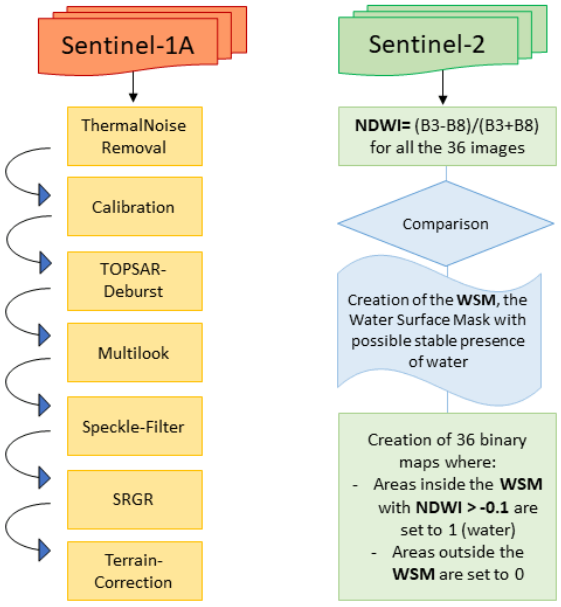

Figure 2: SAR (left) and Multispectral (right) data pre-processing.

4 RESULTS AND DISCUSSION

To carry out the proposed research, we have used an open-source implementation of the U-Net (Wang, 2023). The generated source code has been made publicly available (Galatolo, 2023). Table 2 shows the U-Net hyperparameters settings, achieved via grid search. Figure 5 shows the cross-entropy loss against the iterations. In this image, it can be read that after computing 6000 iterations the system achieves good performances, about 0.013. Figure 6 shows the outputs of the U-Net, one performed on the SAR images and the other one obtained with Multispectral images, both representing the area in the image covered by the water, hereafter called as the "Normalized River Water Extent (NRWE)".

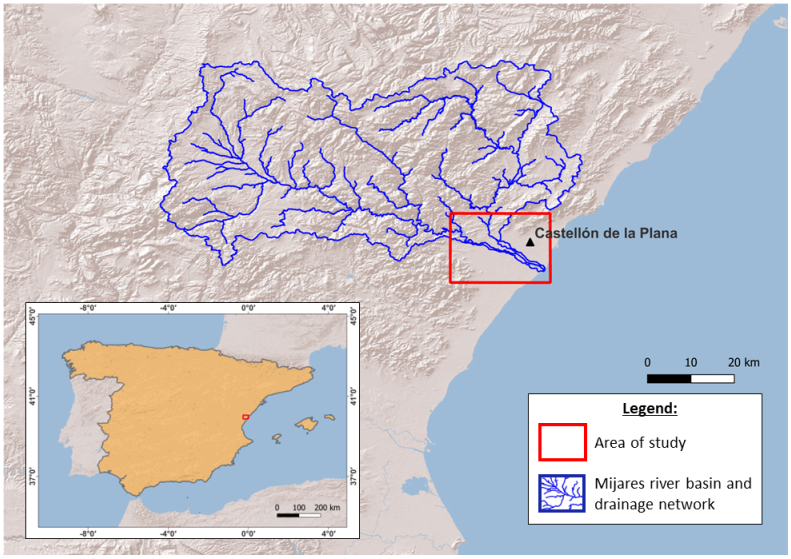

Figure 1: Study area (red rectangle) and river drainage network.

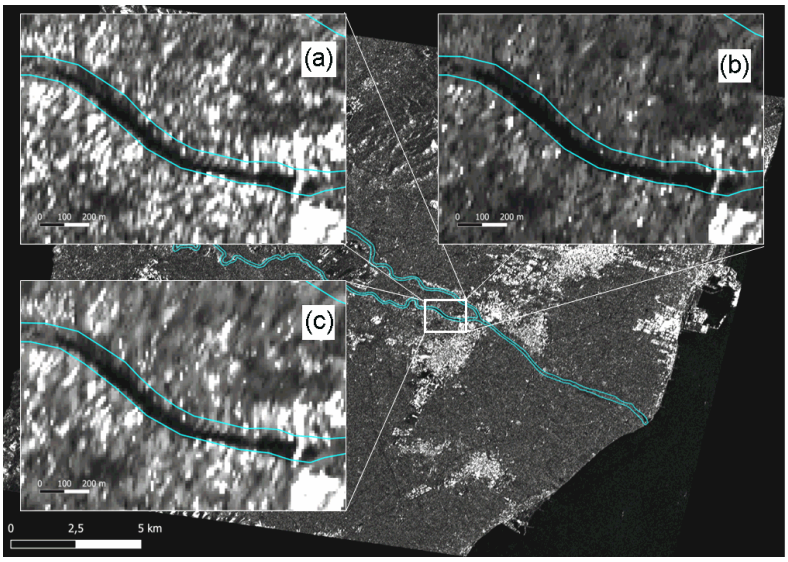

Figure 3: Speckle-Filters, Lee (a), IDAN (b), Lee Sigma (c).

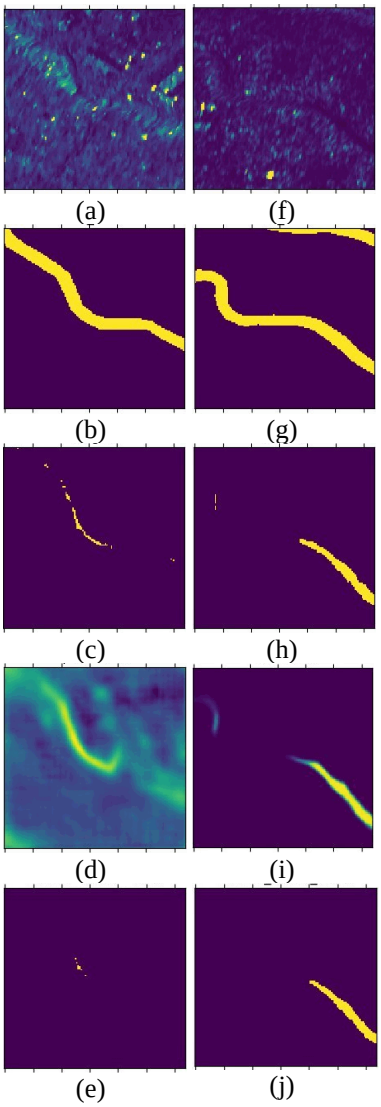

Figure 4: samples after 100 training iterations (a-e), and after 30,000 training iterations (f-j); raw input (a,f); water surface mask (b,g); multispectral bands (c,h); raw output (d,i); discretized output (e,j).

The results obtained using SAR and optical images are promising. Indeed, there is a good similarity between SAR outputs and Optical water masks (Figure 4). Moreover, it can also be appreciated a similar seasonal trend in the NRWE over time. Finally, the Mean Absolute Error (MAE) between the SAR-based NRWE and Optical- based NRWE is 0.072.

5 CONCLUSIONS

In this paper we analysed the Mijares river (Eastern Spain) from April 2019 to September 2022. In particular, we focused on its lower reach that can be considered a challenging task given that this area is often drought prone and it has little detectable water for the most part of the year, yet it registers recurring floods. Differently from the majority of case studies in the literature using remote sensing to map flooding,

wide rivers and large water surfaces, here we used a Convolutional Neural Network for detecting river water surfaces from SAR data, using Multispectral data as a ground truth. Specifically, a data pipeline for satellite data pre-processing is first presented, and then the U-Net architecture is parameterized and trained. The adopted approach, which provided promising early experimental results in the river water surfaces detection through radar backscatter, can be considered as a first step to further investigate the same satellite data sets over a longer period, with the final aim of monitoring the temporal variations and the effects of the climate change in a fragile ecosystem such as rivers. Lastly, to encourage scientific collaborations, the source code used for this work has been made publicly available (Galatolo, 2023).

Table 2: U-Net hyperparameters settings.

Parameter	*Description*	*Value(s)*
dim	no. initial channels	8
dim mults	no. channels multipliers	[1, 2, 4]
blocks per stage	no. convolutional operations per stage	[2, 2, 2]
self-attentions per stage	no. self-attention blocks per stage	[0, 0, 1]
channels	input channels	1
resnet groups	no. normalization groups	2
consolidate upsample fmaps	feature maps consolidation	true
weight standardize	weight standardization	false
attention heads	no. attention heads	2
attention dim head	size of attention head	16
training window size	window size of training samples	128
training batch size	no. of samples per iteration	32
learning rate	amount of weight change in response to the error	0.001

ACKNOWLEDGEMENTS

This work has been partially supported by: (i) the National Center for Sustainable Mobility MOST/Spoke10, funded by the Italian Ministry of University and Research, in the framework of the National Recovery and Resilience Plan; (ii) the PRA_2022_101 project “Decision Support Systems for territorial networks for managing ecosystem services”, funded by the University of Pisa; (iii) the Ministry of University and Research (MUR) as part of the PON 2014-2020 “Research and Innovation" resources – Green/Innovation Action – DM MUR 1061/2022"; (iv) the Italian Ministry of University and Research (MUR), in the framework of the "Reasoning" project, PRIN 2020 LS Programme, Project number 2493 04-11-2021; (v) the Italian Ministry of Education and Research (MIUR) in the framework of the FoReLab project (Departments of Excellence)

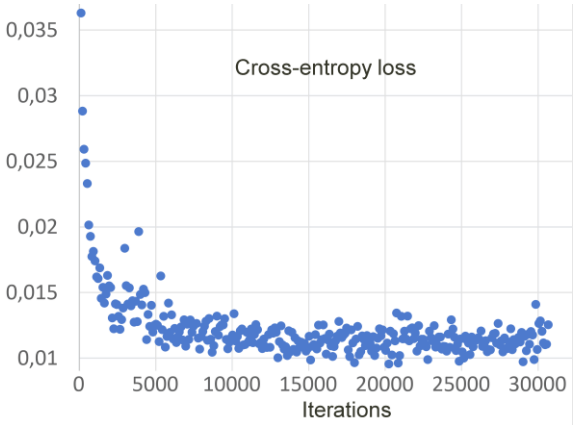

Figure 5: Cross-entropy loss against iterations.

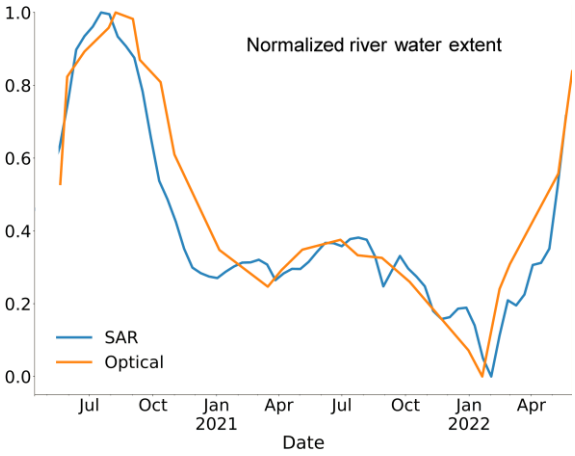

Figure 6: Normalized River Water Extent.

REFERENCES

Botha, E. J., Anstee, J. M., Sagar, S., Lehmann, E., Medeiros, T. A. (2020). Classification of Australian waterbodies across a wide range of optical water types. Remote Sensing, 12(18), 3018.

Carreño-Conde, F., & De Mata Muñoz, M. (2019). Flood monitoring based on the study of Sentinel-1 SAR

images: The Ebro River case study. Water, 11(12), 2454.

Confederación Hidrográfica del Júcar. (2019). Plan Hidrológico de la Demarcación Hidrográfica del Júcar. Revisión de tercer ciclo (2021-2027). https://www.chj.es/es-es/medioambiente/planificacionhidrologica/Paginas/ PHC-2021-2027-Indice.aspx

Filippucci, P., Brocca, L., Bonafoni, S., Saltalippi, C., Wagner, W., & Tarpanelli, A. (2022). Sentinel-2 high-resolution data for river discharge monitoring. Remote Sensing of Environment, 281, 113255.

Frappart, F., Zeiger, P., Betbeder, J., Gond, V., Bellot, R., Baghdadi, N., *et al.* (2021). Automatic detection of inland water bodies along altimetry tracks for estimating surface water storage variations in the Congo Basin. Remote Sensing, 13(19), 3804.

Galatolo F. (2023), GitHub repository, Gistam203, https://github.com/galatolofederico/gistam2023.

Jiang, C., Zhang, H., Wang, C., Ge, J., & Wu, F. (2022). Water Surface Mapping from Sentinel-1 Imagery Based on Attention-UNet3+: A Case Study of Poyang Lake Region. Remote Sensing, 14(19), 4708.

Macian-Sorribes H., Pulido-Velazquez M., and Tilmant A. (2015) Definition of efficient scarcity-based water pricing policies through stochastic programming. Hydrol. Earth Syst. Sci., 19, 3925–3935, 2015 www.hydrol-earth-syst-sci.net/19/3925/2015 doi:10.5194/hess-19-3925-2015

Masson-Delmotte, V., Zhai, P., Chen, Y., Goldfarb, L., Gomis, M. I., Matthews, J. B. R., Berger, S., Huang, M., Yelekçi, O., Yu, R., Zhou, B., Lonnoy, E., Maycock, T. K., Waterfield, T., Leitzell, K., and Caud, N. (2021). Summary for Policymakers. In Climate Change 2021: The Physical Science Basis. Contribution of Working Group I to the Sixth Assessment Report of the Intergovernmental Panel on Climate Change. In Press. www.ipcc.ch

MedECC (2020). Climate and Environmental Change in the Mediterranean Basin – Current Situation and Risks for the Future. First Mediterranean Assessment Report, Cramer, W., Guiot, J., Marini, K. eds., Union for the Mediterranean, Plan Bleu , UNEP/MAP, Marseille, France, 632 pp. ISBN: 978-2-95774146-0-1. DOI 10.5281/zenodo.4768833.

Orlandi, D., Galatolo, F. A., Cimino, M. G., La Rosa, A., Pagli, C., Perilli, N. (2022). Enhancing land subsidence awareness via InSAR data and Deep Transformers. In 2022 IEEE Conference on Cognitive and Computational Aspects of Situation Management (CogSIMA) (pp. 98-103). IEEE.

Pompeu J., I. Ruiz, A. Ruano, H. Bendini and M.J. Sanz (2021) Land use and land cover databases for Mediterranean landscape analysis at the watershed scale. BC3 Working Paper Series 2021-01. Basque Centre for Climate Change (BC3). Leioa, Spain.

Qin, X., Zhang, Z., Huang, C., Dehghan, M., Zaiane, O. R., & Jagersand, M. (2020). U2-Net: Going deeper with nested U-structure for salient object detection. Pattern recognition, 106, 107404.

Quirós, E., & Gagnon, A. S. (2020). Validation of flood risk maps using open source optical and radar satellite imagery. Transactions in GIS, 24(5), 1208-1226.

Ronneberger, O., Fischer, P., & Brox, T. (2015). U-net: Convolutional networks for biomedical image segmentation. In International Conference on Medical image computing and computer-assisted intervention (pp. 234-241). Springer, Cham.

Tran, K. H., Menenti, M., Jia, L. (2022). Surface Water Mapping and Flood Monitoring in the Mekong Delta Using Sentinel-1 SAR Time Series and Otsu Threshold. Remote Sensing, 14(22), 5721.

Wang P. (2023), GitHub repository, Implementation of a U-net complete with efficient attention as well as the latest research findings, https://github.com/lucidrains/x-unet.